Applied Surface Science 506 (2020) 144808

Contents lists available at ScienceDirect

Applied Surface Science

journal homepage: www.elsevier.com/locate/apsusc

Full Length Article

Wavelength effect of ns-pulsed radiation on the reduction of graphene oxide

B.S. de Lima*, M.I.B. Bernardi, V.R. Mastelaro

Sao Carlos Institute of Physics, University of Sao Paulo, 565-905 São Carlos, SP, Brazil

ARTICLE INFO

Keywords:
Photochemical
Photothermal
Reduction
rGO
GO
Wavelength

ABSTRACT

Laser-based methods to reduce of Graphene Oxide (GO) have been pointed out as a promising methodology to produce reduced graphene (rGO) due to its potential for scalable production without the use of chemicals and the processing taking place in ambient conditions. Within this context, this study presents the results of a systematic investigation of the reduction of graphene oxide films by means of an Nd:YAG pulsed laser radiation using wavelengths ranging from Ultra-Violet (UV) to Infra-Red (IR). Our results demonstrated that the reduction carried out using infrared (λ = 1064 nm) and visible radiation (λ = 532 nm) yield higher sp^3-sp^2 conversion as a consequence of photothermal reduction. On the other hand, UV radiation is more efficient in removing oxygen groups due to an enhanced photochemical effect. Furthermore, our results demonstrate that rGO films with C/O ratio greater than 100 can be produced if both photochemical and photothermal effects are present in the reduction process.

1. Introduction

Graphene is a two-dimensional material because it consists of a single layer of carbon atoms that are spatially arranged in a hexagonal symmetry. The atoms are bonded through sp^2 hybridization as in fullerenes, carbon nanotubes or graphite [1]. Interestingly, three σ-electrons participate in the chemical bonding, while the fourth π-electron is the one responsible for electronic transport that could be confined in zero (fullerenes), one (carbon nanotubes), two (graphene), or three (graphite) dimensions. In the case of graphene, it has been shown that its π-electrons have unique properties. For instance, Andre Geim and Kostantine Novoselov, who have isolated graphene through mechanical exfoliation in 2004 [2], experimentally demonstrated that charge transport in graphene is governed by relativistic Dirac equation. Hence it exhibits a linear dispersion relation and quantum Hall effect [3,4]. In 2010, Geim and Novoselov awarded the Nobel Prize in physics due to their work on graphene. As a consequence of these remarkable fundamental properties, graphene also holds the record for electron mobility, thermal conductivity, mechanical tensile strength, and intrinsic surface area [5]. This nanomaterial has been pointed out as an enormous potential for applications in fields such as energy harvesting [6] and storage [7], biosensors [8], and chemical sensors [9,10].

Pristine graphene has been obtained mainly through chemical vapor deposition using hydrocarbon gases as a source of carbon or through graphitization of the surface of SiC single crystals [11]. Both methods operate in temperatures as high as 1000 °C, high vacuum, and require transfer steps that can alter its physical properties [12]. Hence, these methods do not yet provide a technological path for industrial production of graphene-based devices. Within this context, several alternative approaches to produce graphene-related materials have been proposed based on the reduction of Graphene Oxide (GO), because the removal of oxygenated groups restore the graphene properties. For instance, GO exhibit sheet resistance higher than 1×10^4 S cm^{-1} while values in the order of 1×10^3 S cm^{-1} and 400 S cm^{-1} are found for reduced graphene oxide (rGO) and pristine graphene, respectively [13]. Typically, GO is produced via chemical oxidation of graphite layers that are separated by sonication forming stable colloids, like the Hummer's method [14]. Then, these colloids can be reduced via a chemical reaction with strong reducing agents such as hydrazine [13,15]. Also, GO can be reduced by thermal annealing upon heat treatment in temperatures in the order of 1000 °C [16]. Recently, Wang and collaborators demonstrated that rGO with C/O ratio higher than 130 could be achieved with thermal annealing at 3000 K [17].

Within this context, several laser-based methods have been developed to process graphene-related materials [18,19]. Frequently, these methods are pointed out as a potential greener technology to produce high-quality graphene-related devices as the processing takes place under ambient condition and require no chemicals. For instance, UV ns-pulsed laser was used to reduce GO solutions successfully [20]. It has been shown that pulsed CO_2 laser can induce the formation of 3D porous graphene in commercial polyimide [21]. More recently, a study demonstrated that the GO powder could be reduced when irradiated

* Corresponding author.
E-mail address: delima.bs@gmail.com (B.S. de Lima).

https://doi.org/10.1016/j.apsusc.2019.144808
Received 7 August 2019; Received in revised form 14 November 2019; Accepted 19 November 2019
Available online 04 December 2019

with ns pulsed radiation of 355 nm [22]. Regarding ns pulses of infrared (IR) radiation, an interesting paper from Evlashin et al. demonstrated that rGO with oxygen content lower than 3% can be produced by adjusting the laser power and the scanning speed [23]. The use of IR radiation in the reduction of GO has been point out as an efficient manner to decrease defect density in rGO films [24]. IR radiation from CO_2 lasers has been pointed out as very effective radiation to reduce GO films. For instance, Bhattacharjya et al. have produced rGO films with an oxygen content of 1.6% [25]. Ultra-short pulses have also been extensively used to transfer and reduce GO simultaneously [26,27].

It has been proposed that laser-assisted GO reduction is governed by two different mechanisms that depend on the type of light-matter interaction. According to Arul et al. [28], the photochemical reduction is the process in which light interacts with the chemical bonds and remove oxygen functional groups of the surface. This mechanism is mainly activated when GO is irradiated with UV light (typically $\lambda < 400$ nm). Another photoreduction mechanism proposed by Arul et al. takes place under IR radiation ($\lambda > 750$ nm). This process consists of a structural reorganization of GO upon localized temperature rise that may be pictured as carbon sp^3 to sp^2 conversion. This process is usually referred to as photothermal reduction or graphenization [28]. Recently, the C sp^3 to sp^2 conversion was studied in detail by Wan et al. using fs IR radiation. They observed that sp^2 content could be finely tuned through laser fluence and scanning speed [29].

Different studies on laser reduction of GO have been conducted using pulsed radiation with remarkable results [20–23,25–30]. There are still, however, a limited number of studies that are dedicated to the investigation of the photochemical and photothermal reduction mechanisms. Within this context, this study reports an experimental investigation on the reduction of GO films using Nd:YAG ns-pulsed laser with different wavelengths. XPS and Raman spectroscopy results suggested that visible and IR radiation have higher sp^3-sp^2 conversion rate while UV light is more efficient in removing oxygenated groups. Furthermore, rGO films with C/O ratio higher than 100 could be achieved by combining both photochemical and photothermal mechanisms.

2. Experimental procedure

2.1. Laser reduction of GO films

GO aqueous solution (1 mg/mL) was purchased from Sigma Aldrich and drop cast in silicon substrates freshly cleaned with piranha solutions. The substrates were kept at 80 °C for water evaporation, and four cycles of 25 μL each were used in the drop-casting procedure. These films covered an area with a diameter of approximately 5 mm. The laser reduction process was carried out in ambient conditions using a Spectron SL400 Nd:YAG laser system operating with 6 ns pulse duration and a repetition rate of 30 Hz in the TEM00 mode without any focusing lens. In order to investigate the influence of the wavelength in the reduction process we have used fundamental radiation (1064 nm), second (532 nm), third (355 nm) and forth (266 nm) harmonic radiation generated by non-linear type I potassium dideteurium crystals followed by dichroic mirrors that have maximum reflectivity for each of the wavelengths used in order to separate the desired radiation. The beam diameter was approximately 5 mm, and the energy of the beam was kept in the maximum value below any ablation was detected by the naked eye. The ablation fluence for each wavelength is estimated in 380, 150, 85, and 50 mJ/cm^2 for 1064, 532, 355, and 266 nm, respectively. The laser beam scanned a squared area of 20x10 mm at a rate of 1 mm/s with a space between each scan line of 0.25 mm. The scanning was necessary to guarantee that the point of the beam with the highest intensity would interact with the whole sample and to avoid ablation over time due to sample overheating. Each Si substrate with the GO films was kept in the center of this area, and the scanning process was carried out five times to maximize the reduction effect of each radiation and to produce homogeneous films.

2.2. GO and rGO characterization

X-ray diffraction data were collected in a Rigaku Ultima IV diffractometer within the range of $2\theta = 20$ to 60° using Cu-Kα radiation ($\lambda = 1.5418$ Å) and LiF (1 0 0) monochromator in the conventional θ-2θ configuration. Raman spectra were measured in a Witec (Ulm, Germany) microscope equipped with a highly linear stage and objective lens from Nikon (100 × NA = 0.9). Raman signals of our samples were excited with an Nd:YAG laser (532 nm; 10 mW) and Raman light was detected by high sensitivity, back-illuminated Peltier-cooled CCD behind a 600 grooves/mm grating. The data were recorded in the wavenumber range from 600 to 3600 cm^{-1}. All measurements were carried out at room temperature. X-ray Photoelectron Spectroscopy (XPS) measurements were carried out in Scientia Omicron ESCA spectrometer with monochromatic X-ray source Al-Kα (1486.7 eV, with the power of 280 W and a constant pass energy mode of 50 eV). The XPS peaks were fitted using a Voigt function after subtracting a Shirley background. In the fitting procedure, FWHM values were fixed equal to the C-sp^2 component while the position of each peak was allowed to change 0.5 eV in the binding energy.

3. Results and discussion

3.1. GO characterization

To study the effect of wavelength on the laser reduction of GO, let us first discuss the main features of our starting material. Fig. 1(a) and (b) present the XPS chemical surface analysis of a GO film before any laser irradiation. In the survey spectrum, Fig. 1(a), the peaks observed at 532, 400, 285, 232, 169, and 18 were assigned to O 1s, N 1s, C 1s, S 2s, S 2p, and S 3s. According to these results, the C and O contents were 68.28 and 27.51%, respectively, which grants a starting C/O ratio of 2.48. N and S contents were measured as 0.52 and 3.69%, respectively. The XPS survey results of all samples discussed in this report are summarized in Table 1. Fig. 1(b) shows the high-resolution C 1s peak of this GO film. This peak was deconvoluted into C-sp^2 (284.5 eV, reference), C sp^3 (285 eV), epoxide (286.9 eV), carbonyl (288 eV), and carboxyl groups (289 eV). The C-C components represent 34.3% of the chemical states, while C-O represents 65.7%. The results regarding the content of C1s components are summarized in Table 2. Fig. 1(c) presents a typical Raman spectrum obtained from GO films. The most important features discussed in this manuscript are related to the relative intensities of the D, G, and 2D bands, which are highlighted in this Figure.

The D band (~1350 cm^{-1}) is related to defects in the graphene structure, such as vacancies. The D' band (~1610 cm^{-1}) should not be present in few-layer graphene, and a decrease in its intensity has been pointed out as direct evidence of GO reduction [31]. The G band (~1580 cm^{-1}) is related to the vibration of C-sp^2 planes, while the 2D band (~2700 cm^{-1}) is associated with the resonant electronic band structure of graphene [32,33]. The intensity of D and 2D bands relative to the intensity of the G band, namely I_D/I_G and I_{2D}/I_G, are two parameters commonly used to quantify the quality of graphene-related materials. During the reduction process, an increase in the relative intensity of G and 2D bands (measured by a decrease in I_D/I_G and an increase in the I_{2D}/I_G) is attributed to the growth of sp^2 carbon in the hexagonal structure of graphene layers. Furthermore, the ratio I_{2D}/I_G is often used to determine the number of graphene layers. Ideally, single-layer pristine graphene should have $I_D = 0$ and $I_{2D}/I_G = 2$. Our starting GO film exhibits $I_D/I_G = 1.81$ and $I_{2D}/I_G = 0.17$.

3.2. Characterization of laser reduced GO (rGO) with different wavelengths

The influence of photon energy in the reduction of GO studied through XPS analysis were carried out in samples irradiated with the laser with different wavelengths, from infra-red to ultra-violet. Figs. 2

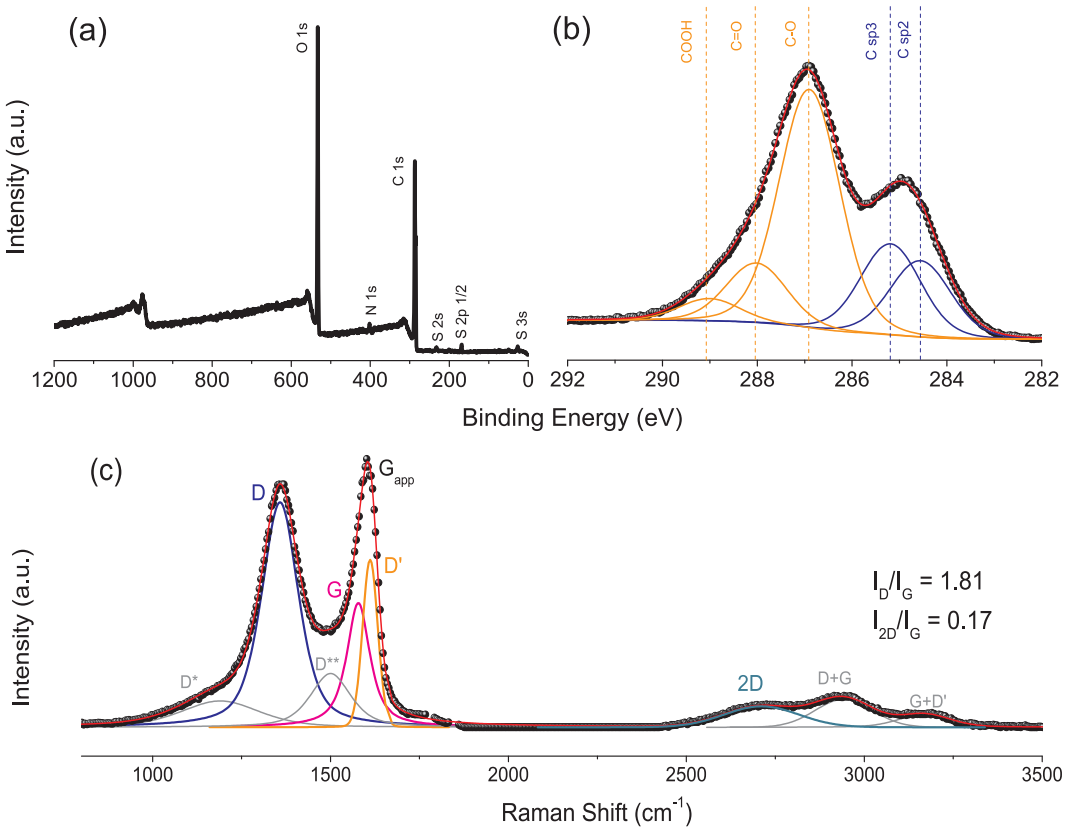

Fig. 1. Typical XPS and Raman spectra of GO films. XPS (a) Survey, (b) high-resolution C 1s, and (c) Raman spectra.

Table 1
Elemental content (%) of GO and rGO films using different wavelengths.

	O	C	S	N	C/O
Graphene Oxide	27.51	68.28	3.69	0.52	2.48
1064	3.68	94.44	1.88	0	25.66
532	8.89	89.04	2.07	0	10.01
355	1.74	98.26	0	0	56.47
266	1.25	98.75	0	0	79.00
266/1064	0.94	99.06	0	0	105.38

Table 2
Content of the components (%) of GO and rGO films using different wavelengths.

	C sp2	C sp3	C-O	C = O	COOH
Graphene Oxide	15.65	18.64	48.91	12.23	4.57
1064	46.36	36.53	10.95	4.35	1.81
532	42.21	32.78	15.64	5.75	3.62
355	44.69	38.62	10.93	3.55	2.21
266	45.41	38.42	10.5	3.67	2
266/1064	48.02	37.52	10.3	2.72	1.44

and 3 show the XPS results of four laser-reduced samples with 1064, 532, 355, and 266 nm wavelengths. The intensity of the O 1s peak observed in the vicinity of 532 eV is significantly smaller than the intensity of O 1s peak found in GO, shown in Fig. 1(a). After the reduction, the amount of carbon in these samples is estimated at 94.44, 89.04, 98.26, and 98.75% to 1064, 532, 355, and 266 nm, respectively. The results regarding the reduction using 1064 nm radiation (~3.7% of remaining oxygen) are in agreement with a previous report from Evlashin *et al.* [23], in which they achieved remaining oxygen content lower than 3% by using the same wavelength. Besides the significant decrease of the O 1s peak intensity, the peaks related to N and S

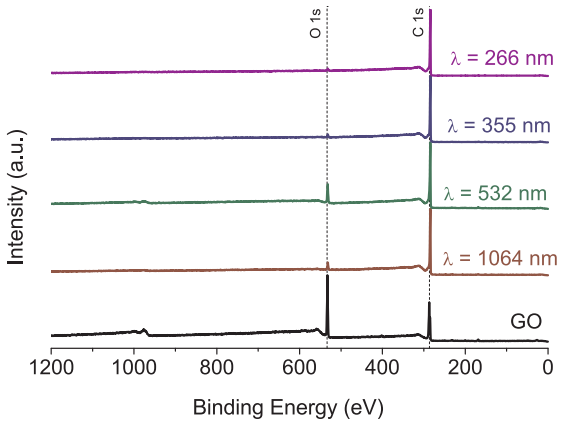

Fig. 2. XPS survey spectra of laser-reduced GO films with different wavelengths.

completely vanished from samples exposed to 1064, 355, and 266 nm. The elemental analysis of these samples made using the XPS survey spectra is summarized in Table 1. Regarding the C 1s high-resolution spectrum of rGO samples, data shown in Fig. 3, the component observed at 284.5 eV assigned to C-sp^2, increased significantly for all samples. The sample 1064-rGO exhibits the highest value of this component (46.4%), followed by the two UV reduced samples 355-rGO (44.7%), and 266-rGO (45.4%). 532-rGO showed the smallest value (42.2%). Regarding the component observed at 285 eV assigned to C-sp^3, also increased significantly. Interestingly, in this case, the sample that showed a higher value was the one reduced with UV radiation. For this component, the results were 36.5, 32.8, 38.6, and 38.4% for 1064, 532, 355, and 266 nm. Finally, the C-Ox components represented 17.1, 25, 16.7, and 16.2% for 1064, 532, 355, and 266 nm reduced GO, respectively. From these results, one can observe that the sample with the

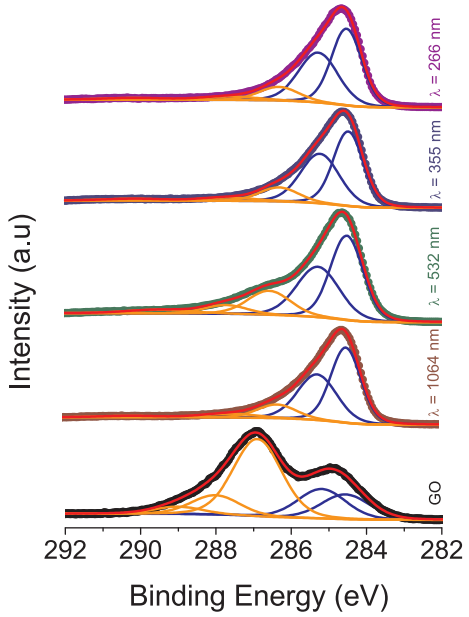

Fig. 3. C 1s high-resolution spectra of laser-reduced GO films with different wavelengths.

highest sp^3-sp^2 conversion rate is the one reduced with IR radiation (1064-rGO), the one with the highest removal of oxygenating groups is the one reduced with UV radiation (266-rGO). Regarding the C/O ratio, the samples reduced with UV light exhibit C/O = 56.5 and 79 for 355-rGO and 266-rGO, respectively, against C/O = 25 and 10 for 1064-rGO and 532-rGO respectively. According to Arul et al. [28], UV light is more efficient in reducing the oxygenated groups content from GO while IR radiation is more effective in the sp^2 structure restoration, which strongly agrees with the results discussed presented in Figs. 2 and 3.

Fig. 4 presents the Raman spectra obtained from samples reduced with different wavelengths to further characterize the effect of the wavelength on the rGO structure. First, one should note that for all rGO

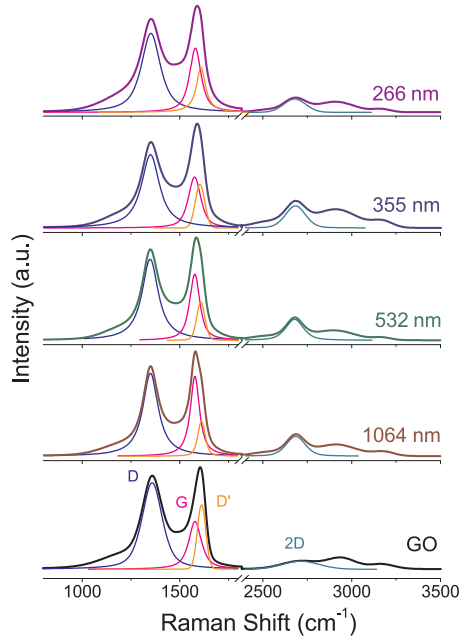

Fig. 4. Comparison of Raman spectra of laser-reduced GO films with different wavelengths.

Table 3
Raman characterization of GO and rGO films using different wavelengths.

	Position-FWHM (cm^{-1})			I_D/I_G	I_{2D}/I_G
	D	G	2D		
Graphene Oxide	1358–122	1578–77	2711–247	1.81	0.17
1064	1349–95	1577–57	2684–125	1.04	0.25
532	1347–100	1576–61	2678–118	1.22	0.32
355	1349–112	1575–76	2683–132	1.44	0.43
266	1351–117	1579–70	2679–145	1.22	0.21
266/1064	1345–80	1571–46	2676–106	0.69	0.27

samples the intensity of the D band did not change significantly relative to the intensity of the apparent G band (result of deconvolution of G and D' bands), suggesting that the laser reduction process did not increase the defects density of the GO structure and hence was kept under the ablation limit. It is possible to observe that the relative intensity of the G band, which is related to the in-plane C-sp^2 vibration, increased significantly for all samples if compared to that of GO. The 1064-rGO sample showed the lowest value (1.04) for I_D/I_G, while this ratio was found to be 1.22, 1.44, 1.23, and 1.81 for 532, 355, 266-rGO, and GO respectively, please check Table 3. This is a key parameter to evaluate both photothermal and photochemical aspects of the GO photoreduction. It is important to mention that our laser reduction experiments were carried out using high-intensity laser and, therefore, local heating is expected for all wavelengths. If one considers that sp^2 structure restoration is the reduction mechanism activated due to local temperature rise, the GO samples reduced with wavelengths that are not absorbed by the C-O bonds should exhibit the highest increase in the relative intensity of the G band. This is the case of 1064 and 532-rGO, which showed the lowest values I_D/I_G.

Interestingly, both samples showed the highest oxygen content of 3.68 and 8.89%, respectively, according to Table 1. Now, if the hypothesis of local heating cannot be ruled out for UV-laser radiation, the reduction mechanism observed for the 355-rGO, and 266-rGO samples should have a photothermal and a photochemical contribution. If a localized temperature rise is partially responsible for the effective reduction of these samples, it could not solely explain the low oxygen content of both samples. While these samples showed the lowest values of I_D/I_G, they were the ones that showed the highest degree of reduction with 1.74 and 1.25% of oxygen. Another interesting feature that should be discussed is the significant increase in the relative intensity of the 2D band. The relative intensity of this band with regards to the G band has changed from 0.17 (GO) to 0.25, 0.32, 0.43, and 0.21 for 1064, 532, 355, and 266-rGO, respectively. The FWHM of this band also decreased significantly from 247 to ~ 130 cm^{-1} for GO and laser rGO. The presence of a sharper and more intensity 2D band is experimental evidence of small disorder in the rGO structure [34]. Another interesting feature that should be evaluated is the crystalline size (L_a) that can be calculated according to the study of Cançado et al. [35]. The L_a increased from 9.3 nm in GO to 16.2, 13.7, 11.63, and 13.62 nm for 1064, 532, 355, and 266-rGO, which also shows that IR radiation is more efficient in graphene structural restoration than UV radiation.

3.3. Photochemical followed by photothermal laser reduction of GO

Now, let us turn the discussion to the results of a sample prepared first by illuminating it with 266 nm laser followed by 1064 nm laser radiation. These results are presented in Fig. 5. One can observe in Fig. 5(a) that the peak related to O 1s (532 eV) have decreased when compared to the GO sample shown in Fig. 1. Here, the oxygen accounts for 0.96% of the elemental content, while C 1s (285 eV) represents 99.04%. To our best knowledge, this is the lowest oxygen content achieved by laser-assisted reduction of GO. As expected, peaks related to N and S were not identified in this sample. Fig. 5(b) shows the C 1s

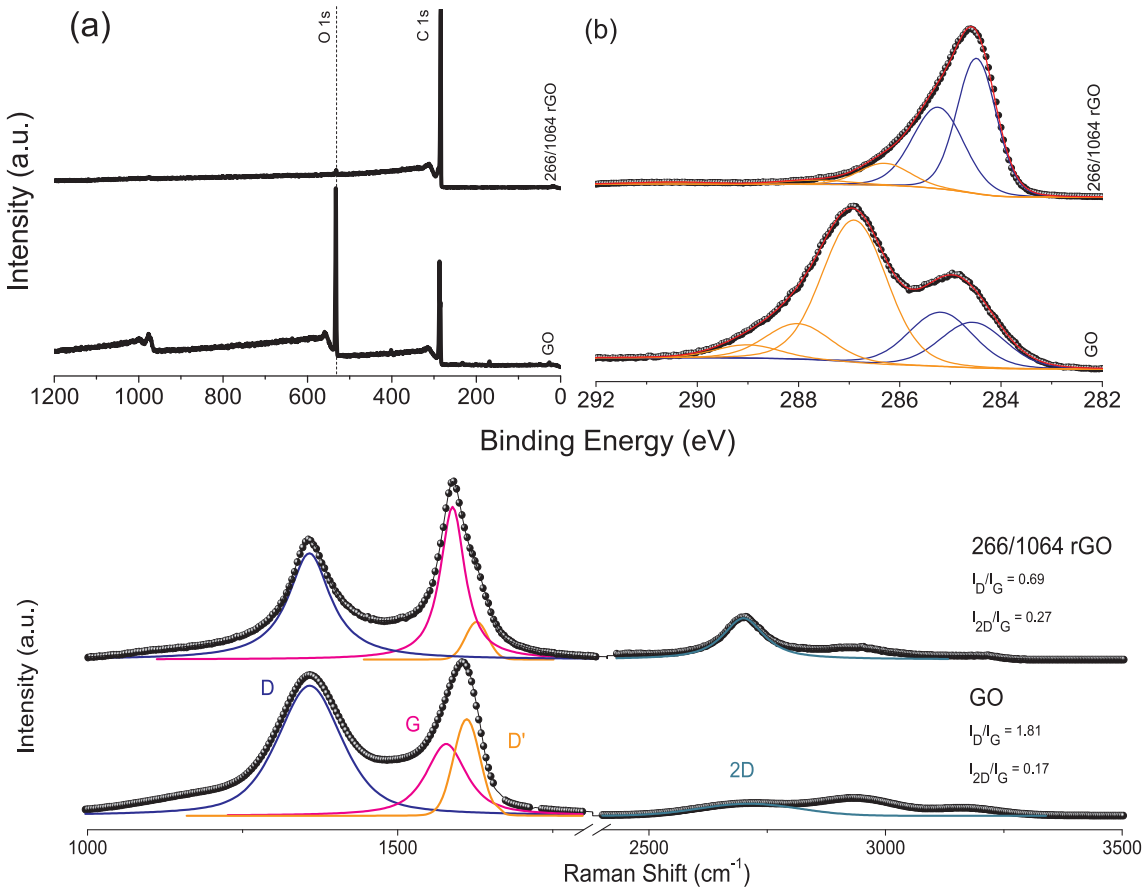

Fig. 5. XPS and Raman spectra comparison of GO and laser rGO using photochemical followed by photothermal reduction.

high-resolution spectrum of this sample. This sample showed the highest content of C-sp^2 (48%) and C-sp^3 (37.5%), and the lowest materials of epoxide (10.3%), carbonyl (2.7%), and carboxyl groups (1.4%). Hence, the C-C components represent 85.5% of the chemical states, while C-O represents 14.5%, please check Table 2. Fig. 5(c) presents the Raman spectra of original GO and rGO obtained through illumination with 266 and 1064 nm respectively. Both values changed significantly from GO sample shown in Fig. 1(c) and from 266-rGO showed in Fig. 4.

The relative intensity of G and 2D bands of the sample reduced with both UV and IR radiations were the highest observed from all samples of the present study, which strongly suggests that the graphene C-sp^2 structure can be restored even further using both UV and IR radiations. In other words, the significant increase in the relative intensity of G and 2D bands shows that the IR radiation may be used to restore the sp^2 C structure of a highly reduced GO with UV light.

X-ray diffraction can be used to estimate the average distance of GO and rGO layers from the position of the peak observed in the θ-2θ diffraction pattern. This peak is indirectly related to the number of oxygen groups bonded to the GO molecule. Fig. 6 presents the XRD data obtained from GO samples reduced with 266 nm radiation (red line) and another that was further reduced with 1064 nm radiation (blue line). The peak is centered in 2θ = 10.13, 10.38, and 11°, respectively. These results indicate that the GO layer distances decreased from 8.7 to 8.5 Å when the GO is irradiated with 266 nm radiation and the distance decrease to 8 Å. It is important to mention that samples prepared with 1064, 532, and 355 nm radiation exhibit the diffraction peak in the vicinity of 2θ = 10.4° (data not shown), which results in the distance between layers of 8.5 Å.

Another interesting feature that should be noted in laser rGO films prepared in this study is the laser-induced periodic surface structure

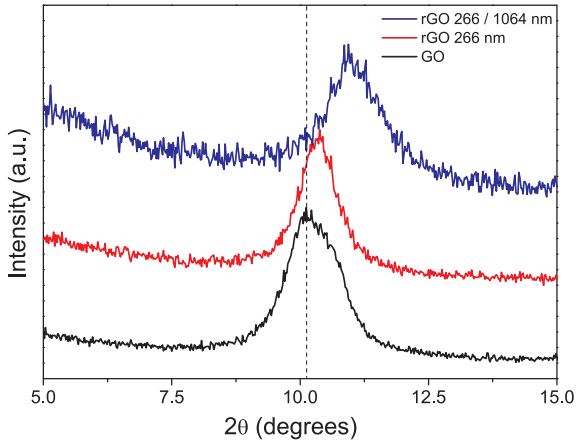

Fig. 6. XRD analysis of GO and laser rGO with different wavelengths.

(LIPSS). Fig. 7 shows micrographs obtained from GO and laser rGO using radiation at 266 nm, 1064 nm and both wavelenghts. It is important to mention that the surface structuring was observed in samples prepared with any wavelength. The difference between them, however, lies in the average size of the periodic structure formed. It is possible to observe that IR radiation induces larger periodic structures on GO than does UV radiation. Samples prepared by using IR radiation after UV radiation do not show any increase in the size of the periodic structures. Fig. 7(a) shows a typical graphene oxide morphology in which it is possible to observe a smooth sheet-like surface with wrinkles due to the stacking of several GO layers. Fig. 7(b)–(d) show a highly porous rGO structure formed by using 266, 1064 and both 266/1064 nm radiations, respectively. A similar structure has been observed by Yung et al.

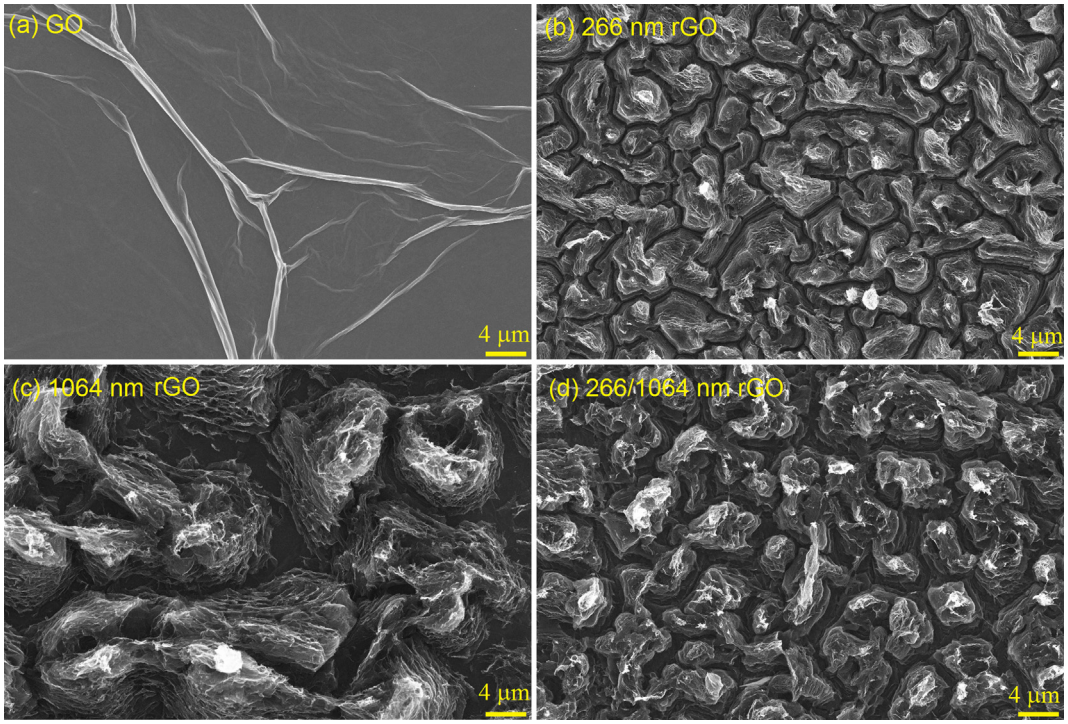

Fig. 7. SEM images of GO and laser rGO films. Microstructure of rGO films shows laser-induced periodic surface structuring.

during laser reduction of graphene oxide with 1064 nm radiation in the same level of fluence (150 mJ/cm^2) of this report. The authors have attributed the formation of this structure to the deoxygenation of the GO layers.

4. Conclusions

This study showed the influence of the wavelength on a laser-assisted reduction of GO. Our results demonstrate that laser reduction of GO with UV light is more effective in decreasing the oxygen content of GO, although less effective in the conversion to the typical sp^2 carbon structure of graphene. This is known as the photochemical reduction mechanism. Furthermore, our results confirm that the IR laser reduces GO mainly due to a local temperature rise that converts more efficiently C-sp^3 to C-sp^2, the so-called photothermal reduction mechanism. By keeping the laser intensity just under the ablation limit and processing GO films with two different wavelengths, we have demonstrated that ns-pulsed laser 266 nm radiation can efficiently remove oxygen groups and while 1064 nm radiation can efficiently restore C-sp^2, granting an oxygen content of less than 1%. To our best knowledge, this is the lowest oxygen content obtained through laser-assisted reduction methods in the literature of GO. Furthermore, our results open new perspectives to explore the other laser processing parameters such as pulse duration, repetition rate, and scanning speed with different wavelengths.

Declaration of Competing Interest

The authors declare that they have no known competing financial interests or personal relationships that could have appeared to influence the work reported in this paper.

Acknowledgements

This work was supported by Fundação de Amparo à Pesquisa do Estado de São Paulo – FAPESP (Grants nº 2018/07517-2 and 2013/07296-2). The authors are thankful to Mauricio A. M. Jr and Thalles T. A. Lucas for the discussions on the reduction mechanisms of graphene oxide.

References

[1] A. Hirsch, The era of carbon allotropes, Nat. Mater. 9 (11) (2010) 868–871.
[2] K.S. Novoselov, A.K. Geim, S.V. Morozov, D. Jiang, Y. Zhang, S.V. Dubonos, I.V. Grigorieva, A.A. Firsov, Electric field effect in atomically thin carbon films, Science 306 (5696) (2004) 666–669.
[3] K.S. Novoselov, A.K. Geim, S.V. Morozov, D. Jiang, M.I. Katsnelson, I.V. Grigorieva, S.V. Dubonos, A.A. Firsov, Two-dimensional gas of massless dirac fermions in graphene, Nature 438 (7065) (2005) 197–200.
[4] A.H. Castro Neto, F. Guinea, N.M.R. Peres, K.S. Novoselov, A.K. Geim, The electronic properties of graphene, Rev. Modern Phys. 81 (1) (2009) 109–162.
[5] N. Savage, Materials science super carbon, Nature 483 (7389) (2012) S30.
[6] J.P.G. Tarelho, M.P.S. Dos Santos, J.A.F. Ferreira, A. Ramos, S. Kopyl, S.O. Kim, S. Hong, A. Kholkin, Graphene-based materials and structures for energy harvesting with fluids - a review, Mater. Today 21 (10) (2018) 1019–1041.
[7] S.I. Wong, J. Sunarso, B.T. Wong, H. Lin, A.M. Yu, B.H. Jia, Towards enhanced energy density of graphene-based supercapacitors: current status approaches, and future directions, J. Power Sources 396 (2018) 182–206.
[8] E. Morales-Narvaez, L. Baptista-Pires, A. Zamora-Galvez, A. Merkoci, Graphene-based biosensors: going simple, Adv. Mater. 29 (7) (2017).
[9] F. Schedin, A.K. Geim, S.V. Morozov, E.W. Hill, P. Blake, M.I. Katsnelson, K.S. Novoselov, Detection of individual gas molecules adsorbed on graphene, Nat. Mater. 6 (9) (2007) 652–655.
[10] A. Nag, A. Mitra, S.C. Mukhopadhyay, Graphene and its sensor-based applications: a review, Sensors Actuat. A-Phys. 270 (2018) 177–194.
[11] P. Avouris, C. Dimitrakopoulos, Graphene: synthesis and applications, Mater. Today 15 (3) (2012) 86–97.
[12] A.W. Robertson, C.S. Allen, Y.A. Wu, K. He, J. Olivier, J. Neethling, A.I. Kirkland, J.H. Warner, Spatial control of defect creation in graphene at the nanoscale, Nat. Commun. 3 (2012).
[13] S.F. Pei, H.M. Cheng, The reduction of graphene oxide, Carbon 50 (9) (2012) 3210–3228.
[14] J.P. Zhao, S.F. Pei, W.C. Ren, L.B. Gao, H.M. Cheng, Efficient preparation of large-area graphene oxide sheets for transparent conductive films, ACS Nano 4 (9) (2010) 5245–5252.
[15] C. Yu, C.F. Wang, S. Chen, Facile access to graphene oxide from ferro-induced oxidation, Sci. Rep. 6 (2016).
[16] X.L. Li, H.L. Wang, J.T. Robinson, H. Sanchez, G. Diankov, H.J. Dai, Simultaneous nitrogen doping and reduction of graphene oxide, J. Am. Chem. Soc. 131 (43) (2009) 15939–15944.
[17] Y.L. Wang, Y.A. Chen, S.D. Lacey, L.S. Xu, H. Xie, T. Li, V.A. Danner, L.B. Hu, Reduced graphene oxide film with record-high conductivity and mobility, Mater. Today 21 (2) (2018) 186–192.
[18] R. Kumar, R.K. Singh, D.P. Singh, E. Joanni, R.M. Yadav, S.A. Moshkalev, Laser-

assisted synthesis, reduction and micro-patterning of graphene: recent progress and applications, Coord. Chem. Rev. 342 (2017) 34–79.
[19] Y. Zhao, Q. Han, Z.H. Cheng, L. Jiang, L.T. Qu, Integrated graphene systems by laser irradiation for advanced devices, Nano Today 12 (2017) 14–30.
[20] L. Huang, Y. Liu, L.C. Ji, Y.Q. Xie, T. Wang, W.Z. Shi, Pulsed laser assisted reduction of graphene oxide, Carbon 49 (7) (2011) 2431–2436.
[21] J. Lin, Z.W. Peng, Y.Y. Liu, F. Ruiz-Zepeda, R.Q. Ye, E.L.G. Samuel, M.J. Yacaman, B.I. Yakobson, J.M. Tour, Laser-induced porous graphene films from commercial polymers, Nat. Commun. 5 (2014).
[22] C.R. Yang, S.F. Tseng, Y.T. Chen, Laser-induced reduction of graphene oxide powders by high pulsed ultraviolet laser irradiations, Appl. Surf. Sci. 444 (2018) 578–583.
[23] S.A. Evlashin, S.E. Svyakhovskiy, F.S. Fedorov, Y.A. Mankelevich, P.V. Dyakonov, N.V. Minaev, S.A. Dagesyan, K.I. Maslakov, R.A. Khmelnitsky, N.V. Suetin, I.S. Akhatov, A.G. Nasibulin, Ambient condition production of high quality reduced graphene oxide, Adv. Mater. Interfaces 5 (18) (2018).
[24] A. Antonelou, L. Sygellou, K. Vrettos, V. Georgakilas, S.N. Yannopoulos, Efficient defect healing and ultralow sheet resistance of laser-assisted reduced graphene oxide at ambient conditions, Carbon 139 (2018) 492–499.
[25] D. Bhattacharjya, C.H. Kim, J.H. Kim, I.K. You, J.B. In, S.M. Lee, Fast and controllable reduction of graphene oxide by low-cost Co2 laser for supercapacitor application, Appl. Surf. Sci. 462 (2018) 353–361.
[26] H.Y. Chen, D.D. Han, Y. Tian, R.Q. Shao, S. Wei, Mask-free and programmable patterning of graphene by ultrafast laser direct writing, Chem. Phys. 430 (2014) 13–17.
[27] M. Kasischke, S. Maragkaki, S. Volz, A. Ostendorf, E.L. Gurevich, Simultaneous nanopatterning and reduction of graphene oxide by femtosecond laser pulses, Appl. Surf. Sci. 445 (2018) 197–203.
[28] R. Arul, R.N. Oosterbeek, J. Robertson, G.Y. Xu, J.Y. Jin, M.C. Simpson, The mechanism of direct laser writing of graphene features into graphene oxide films involves photoreduction and thermally assisted structural rearrangement, Carbon 99 (2016) 423–431.
[29] Z.F. Wan, S.J. Wang, B. Haylock, J. Kaur, P. Tanner, D. Thiel, R. Sang, I.S. Cole, X.P. Li, M. Lobino, Q. Li, Tuning the sub-processes in laser reduction of graphene oxide by adjusting the power and scanning speed of laser, Carbon 141 (2019) 83–91.
[30] Y.L. Zhang, L. Guo, H. Xia, Q.D. Chen, J. Feng, H.B. Sun, Photoreduction of graphene oxides: methods, properties, and applications, Adv. Opt. Mater. 2 (1) (2014) 10–28.
[31] A.A.K. King, B.R. Davies, N. Noorbehesht, P. Newman, T.L. Church, A.T. Harris, J.M. Razal, A.I. Minett, A new raman metric for the characterisation of graphene oxide and its derivatives, Sci. Rep. 6 (2016).
[32] R. Muzyka, S. Drewniak, T. Pustelny, M. Chrubasik, G. Gryglewicz, Characterization of graphite oxide and reduced graphene oxide obtained from different graphite precursors and oxidized by different methods using raman spectroscopy, Materials 11 (7) (2018).
[33] A. Kaniyoor, S. Ramaprabhu, A Raman spectroscopic investigation of graphite oxide derived graphene, AIP Adv. 2 (3) (2012).
[34] J.B. Wu, M.L. Lin, X. Cong, H.N. Liu, P.H. Tan, Raman spectroscopy of graphene-based materials and its applications in related devices, Chem. Soc. Rev. 47 (5) (2018) 1822–1873.
[35] L.G. Cancado, K. Takai, T. Enoki, M. Endo, Y.A. Kim, H. Mizusaki, A. Jorio, L.N. Coelho, R. Magalhaes-Paniago, M.A. Pimenta, General equation for the determination of the crystallite size L-A Of nanographite by Raman spectroscopy, Appl. Phys. Lett. 88 (16) (2006).